Supporting Information

Asymmetric AgPd-AuNR heterostructure with enhanced photothermal performance and SERS activity

*Han Zhang, Zeke Liu, Xiaolin Kang, Jun Guo, Wanli Ma, and Si Cheng**

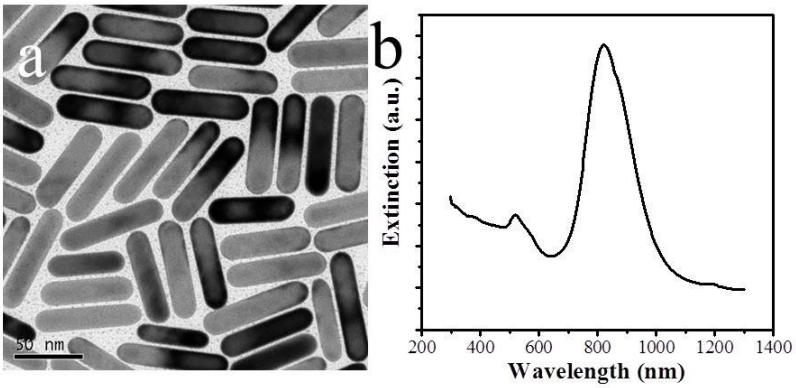

Figure S1. TEM image and extinction spectrum of AuNRs

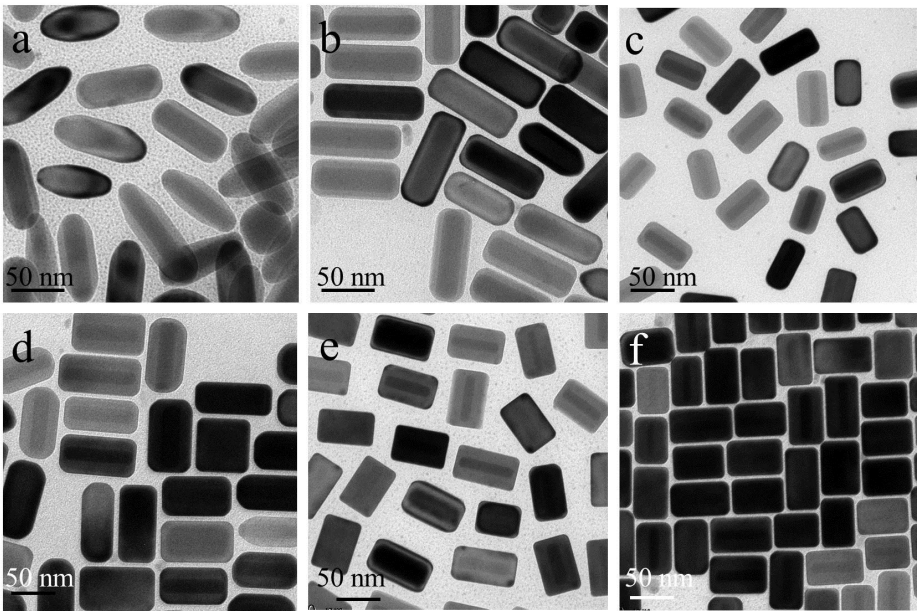

Figure S2. TEM images of AuNRs@Ag core-shell nanostructures with different thicknesses of Ag shell. a) $AgNO_3$ 60 μL. b) $AgNO_3$ 100 μL. c) $AgNO_3$ 200 μL. d) $AgNO_3$ 300 μL. e) $AgNO_3$ 400 μL. f) $AgNO_3$ 500 μL. From a to f, the width of AuNR@Ag nanorods varied from 28.3±1.3 nm, 29.8±1.6 nm, 36.2±1.8 nm, 41.2±2.3 nm, 44.6±2.0 nm to 45.9±3.1 nm.

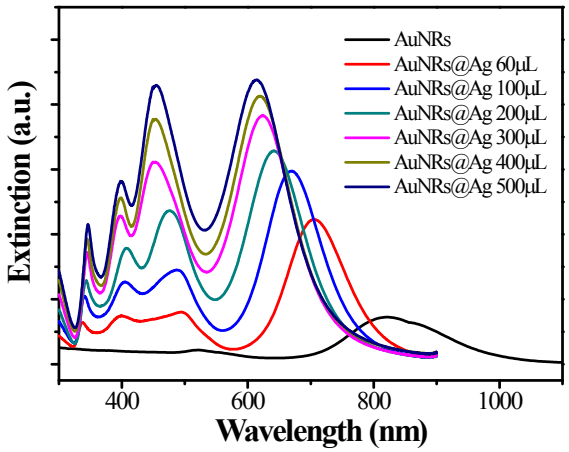

Figure S3. Extinction spectra of AuNRs@Ag core-shell nanostructures with different volume of $AgNO_3$ ranging from 60 μL to 500 μL.

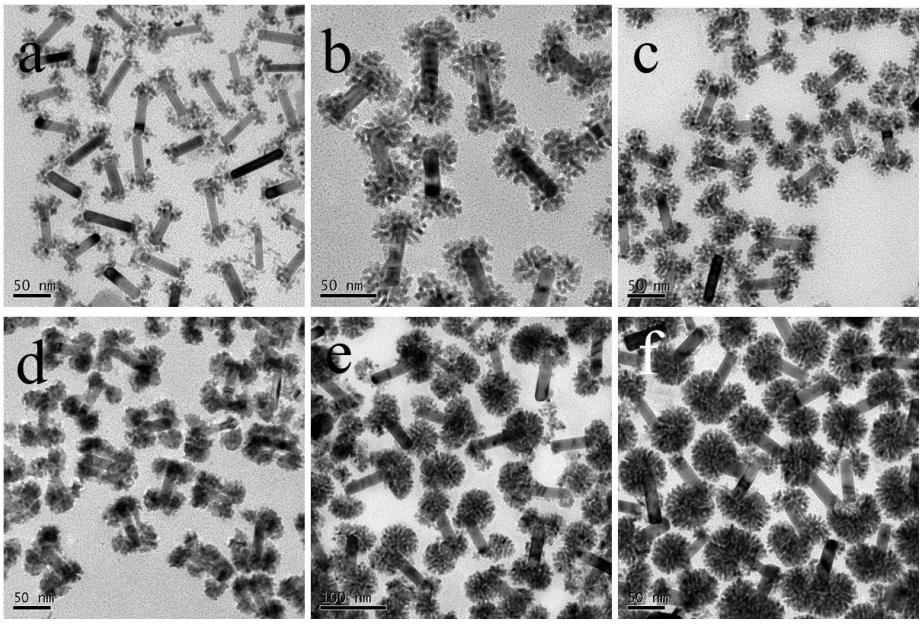

Figure S4.TEM images of AuNRs@AgPd structures prepared with 60 μl (a), 100 μl (b), 200 μl (c), 300 μl (d), 400 μl (e) and 500 μl (f) $AgNO_3$ (0.01 M) solution, respectively.

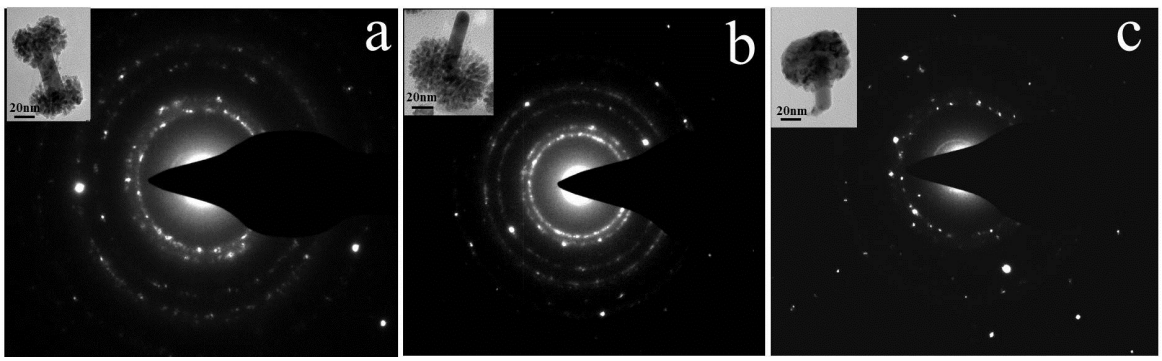

Figure S5. SEAD patterns of nanodumbbell, dandelion and lollipop nanostructures

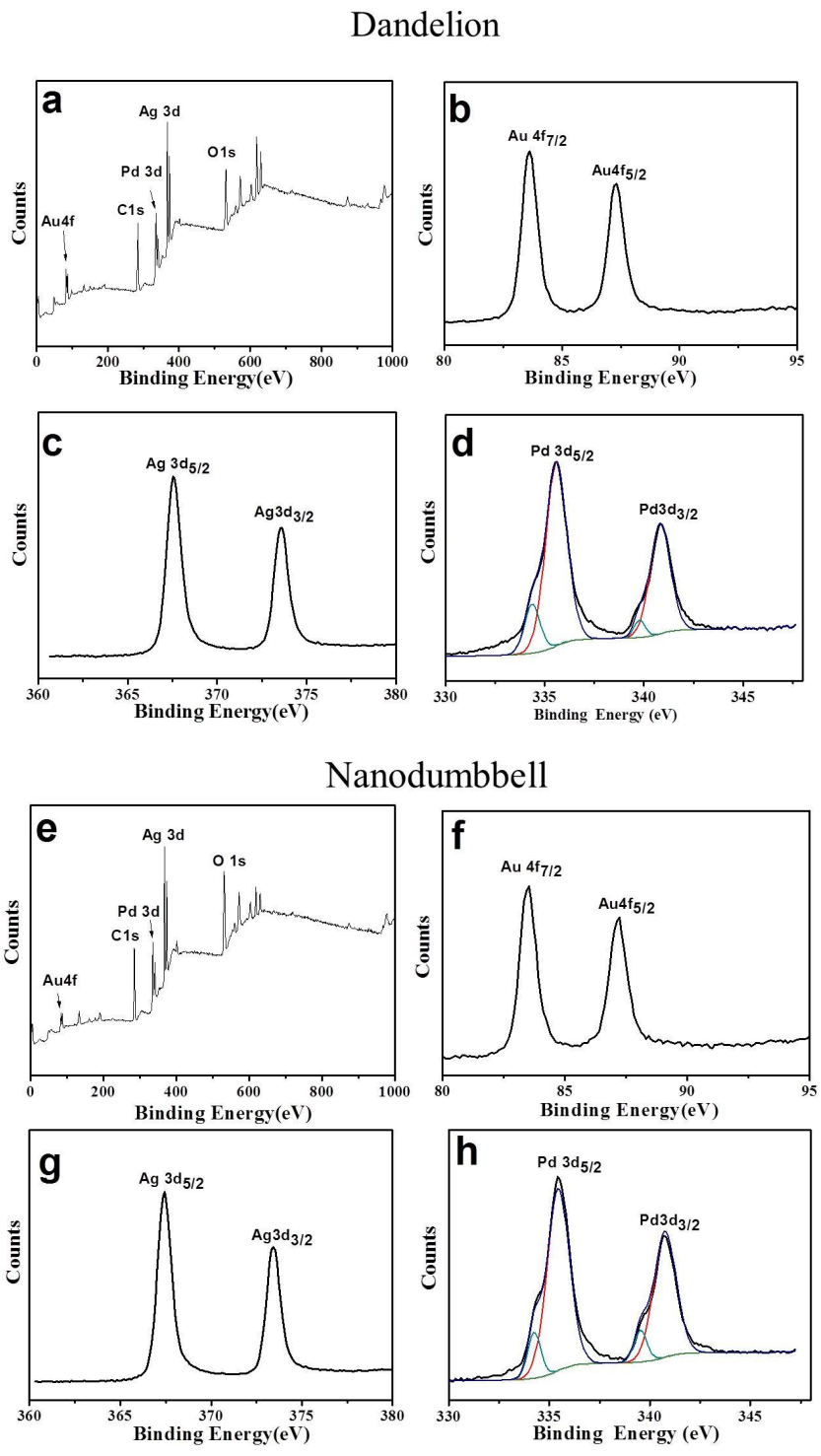

Figure S6. XPS spectra of the dandelion NPs (a-d) and nanodumbbell (e-f). (a,e) Survey spectrum, (b,c,d,f,g, h) the high resolution spectra of Au 4f, Ag 3d and Pd 3d.

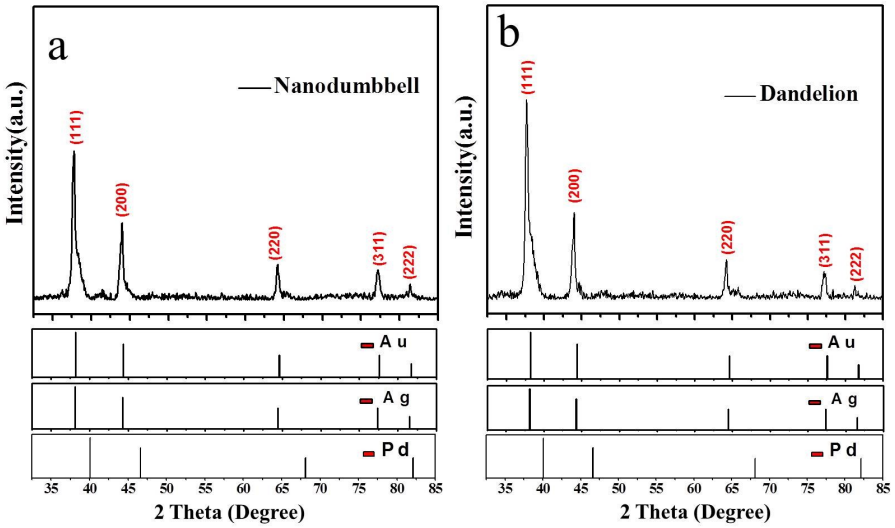

Figure S7 XRD patterns of nanodumbbell (a) and dandelion NPs (b)

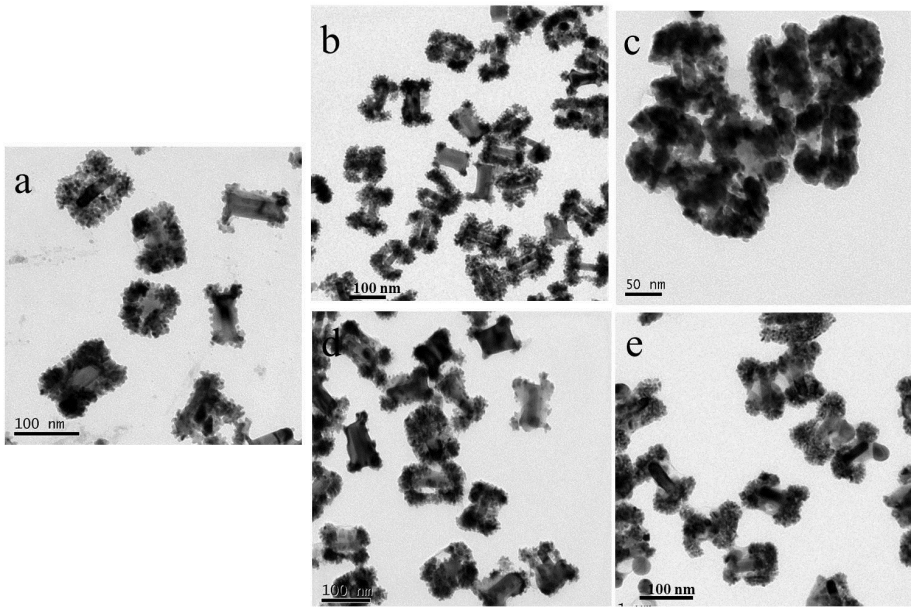

Figure S8. TEM images of AuNRs@AgPd nanostructures with different amount of AA and CTAC. a) no CTAC and no AA. b) no CTAC, 20 μL AA. c) no CTAC, 60 μL AA. d) no AA, 30 μL CTAC. e) no AA, 60 μL CTAC. The volume of $AgNO_3$ is 500 μL.

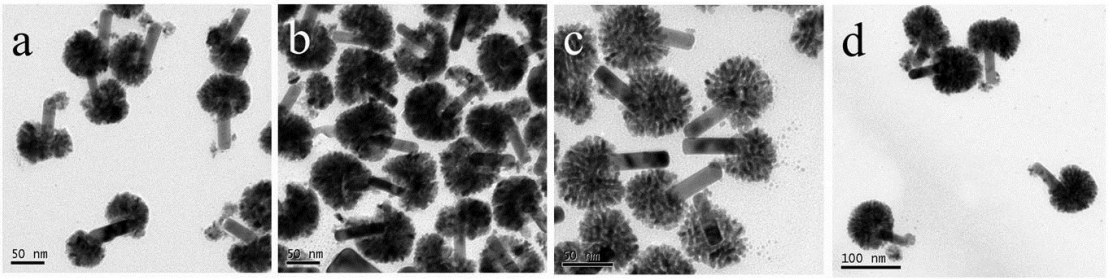

Figure S9. TEM images of AuNRs@AgPd nanostructures with different amount of AA and CTAC. a) 30 μL CTAC and 20 μL AA. b) 30 μL CTAC and 60 μL AA. c) 60 μL CTAC and 20 μL AA. d) 60 μL CTAC and 60 μL AA. The volume of $AgNO_3$ is 500 μL.

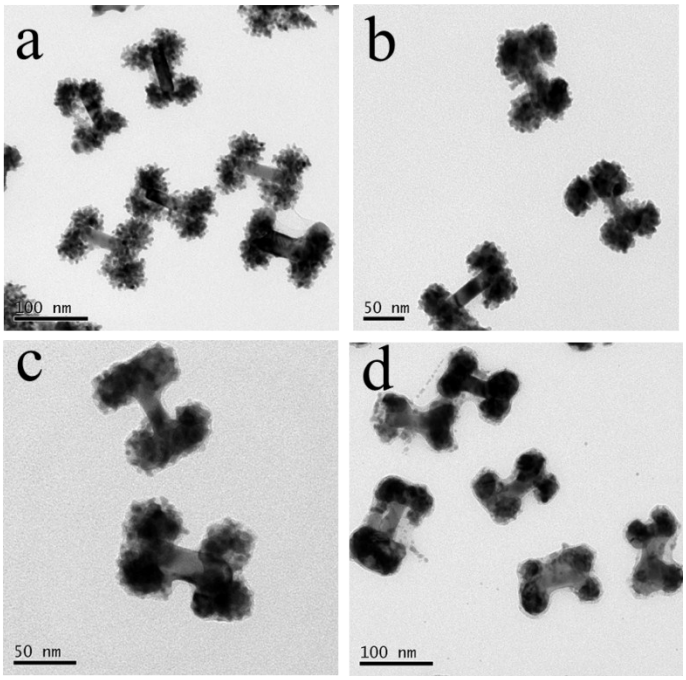

Figure S10. TEM images of AuNRs@AgPd nanodumbbell nanostructures with different amount of AA. a) 20 μL AA. b) 30 μL AA. c) 40 μL AA. d) 60 μL AA. The volume of $AgNO_3$ is 300 μL.

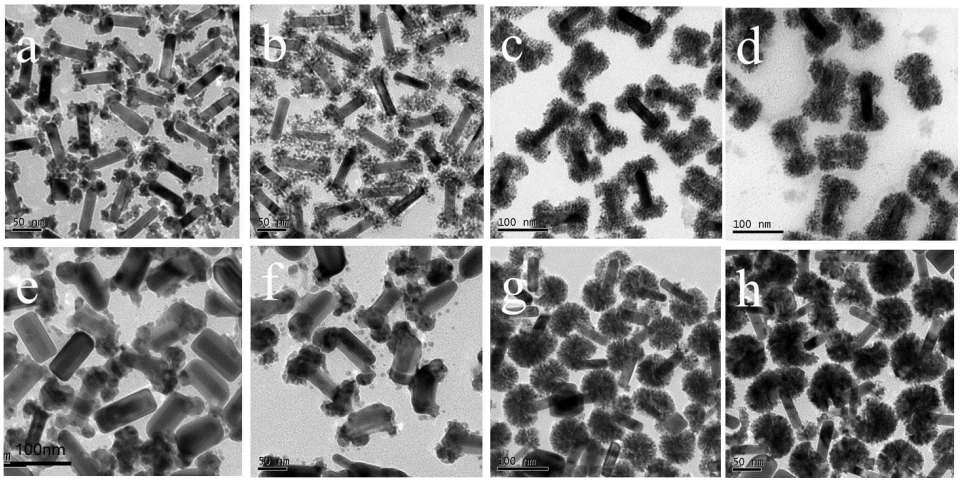

Figure S11. TEM images of nanodumbbell (top) and dandelion (bottom) nanostructures with different amount of H_2PdCl_4. a,e) 10 μL. b,f) 20 μL. c,g) 60 μL. d,h) 80 μL.

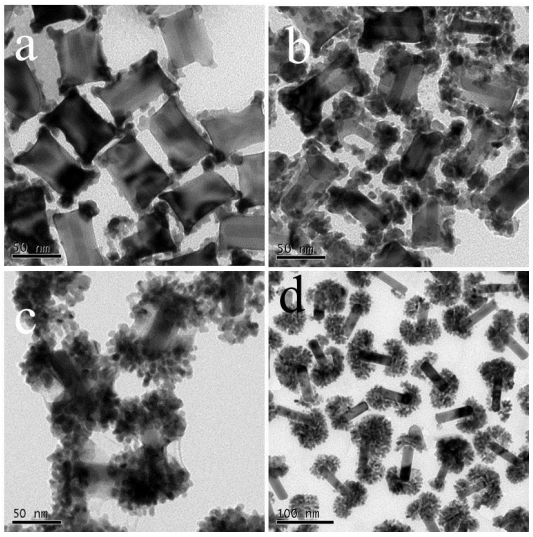

Figure S12. TEM images of AuNRs@AgPd dandelion nanostructures at different reaction stages. a) After the very early Pd precursor injection without additional CTAC and AA. b) 1 min. c) 5 min. d) At high relative ratio of $AgNO_3$. The reaction time is 1h.

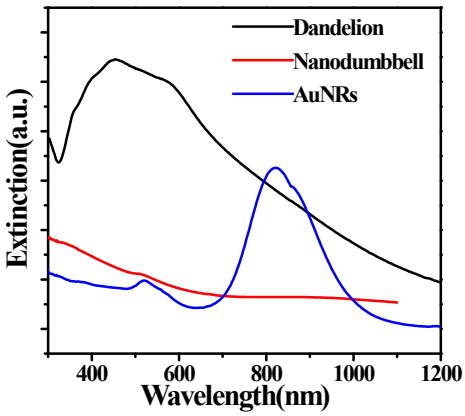

Figure S13. Extinction spectra of gold nanorods, nanodumbbell and dandelion NPs.

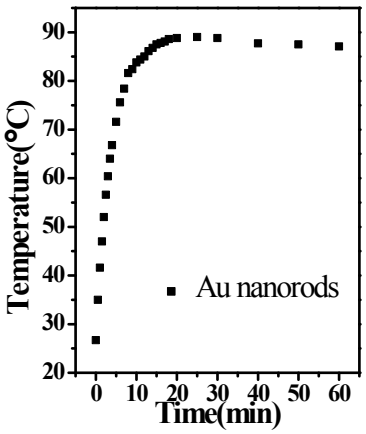

Figure S14. The temperature rise traces of the gold nanorods solution at 1.45 W of the 808 nm laser.

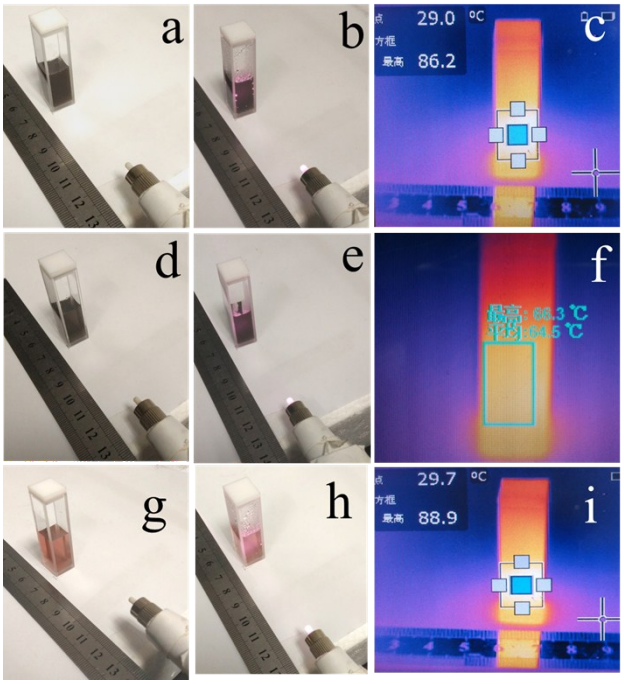

Figure S15. The digital photographs of the dandelion NPs(a-c), nanodummbbell NPs(d-f) and gold nanorods(g-i) solutions before (left), after (middle) illuminated by laser and the digital photographs of final steady-state temperature (righ).

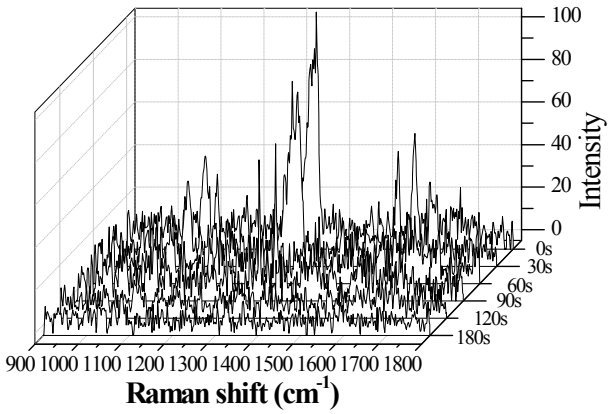

Figure S16. Raman spectra of the reduction of 4-NTP to 4-ATP by nanodumbbell NPs at different reaction time.